Critical dynamics of the λ transition in liquid ^{4}He: Light-scattering spectrum

Richard A. Ferrell and Jayanta K. Bhattacharjee
Institute for Physical Science and Technology and Department of Physics and Astronomy, University of Maryland, College Park, Maryland 20742
(Received 23 March 1979)

From kinetic-theory considerations a general expression is derived for the frequency-dependent critical thermal conductivity of liquid ^{4}He near its λ point. Adding the transient solutions yields an expression for the temperature- and frequency-dependent entropy relaxation rate which includes the corrections to dynamic scaling. This is used to study the fluctuation spectrum at and above the λ point. A detailed comparison with the light scattering data of Tarvin, Vidal, and Greytak yields good agreement.

I. INTRODUCTION

The dynamic-scaling theory[1,2] when applied to liquid helium predicts a divergence in the thermal conductivity and second-sound damping as the λ point is approached from above and below, respectively. In each case the divergence follows a $t^{-1/3}$ law, where $t = |T - T_\lambda|/T_\lambda$. The logarithmic variation of the specific heat near the λ point causes the exponent to deviate from the pure scaling value of $\frac{1}{3}$ by about 20%. Divergences agreeing with these power laws were observed in the experiments of Ahlers[3] and Tyson.[4] However, a later more precise measurement of the thermal conductivity by Ahlers[5] very close to the λ point indicated a definite deviation from the scaling prediction. It was found that the divergence was stronger than that predicted by dynamic scaling (when due account was taken of the specific heat).

A further test of the dynamic-scaling theory is provided by the light scattering experiments. Above the λ point the spectrum is expected to be nearly Lorentzian, with the half-width determined by the thermal conductivity. Thus the spectrum should shrink as one leaves the critical region according to the dynamic-scaling law. Below the λ point this behavior is to be expected for the width of the second-sound doublet. The experimental findings of Tarvin, Vidal, and Greytak[6] and of Vinen *et al.*[7] do not show these features. Above the λ point the spectrum hardly changes its width, while below, the breadth of the second-sound lines falls slightly at first and then rises slowly.

It was found by De Dominicis and Peliti[8] that there was the possibility of a violation of scaling in liquid helium. The Sasvàri-Schwabl-Szégpfalusy[9] (SSS) model with an n-component nonconserved order-parameter field of $O(n)$ symmetry and an $n(n-1)/2$ component conserved generator field of rotations was studied in detail by De Dominicis and Peliti,[10] Dohm and Ferrell,[11] and the present authors.[12] It was found that there exists a curve in the n-D plane along which the order-parameter relaxation rate is vanishingly small when compared to the rate for the generator. This boundary curve was calculated to two-loop order and it was established that, although liquid helium ($n = 2, D = 3$) is on the scaling side, it is very close to the boundary. This led to the characterization of helium by a small value of the ratio w of the relaxation rates. According to Dohm[13] and the present authors[12] $w = O(0.1)$.

A characteristic feature of a small w is the existence of a "slow" transient, i.e., a correction to scaling with a small exponent. The smallness of the exponent causes this correction term to persist deep down into the critical region. The true critical region thus becomes practically inaccessible. It was recently shown by the authors[14] that, when the corrections to scaling are taken into account, an excellent fit to the Ahlers[5] thermal-conductivity data can be obtained. The picture that emerges from that work is the following: Coming from the scaling region, the thermal conductivity is reduced from its true scaling value by the "slow transient" and is then prevented from further decrease by the "fast transient." It finally merges into a constant background value. The Onsager coefficient for the order parameter, on the other hand, has a correction of the opposite sign. This is because its scaling behavior, with an anomalously small numerical coefficient, has to match, by means of the transients, on to a noncritical background value of the same order of magnitude as the background entropy diffusion constant. We also found[14] that these considerations can explain the light scattering data.

In Sec. II of this paper we give a derivation for the critical part of the thermal conductivity. This is generalized to a frequency-dependent form in Sec. III where we also show how the frequency dependence is closely related to the temperature dependence. This connection enables us to describe the two aspects with one combined scaling variable. It is possible to extract the frequency dependence that is required for

an analysis of the entropy fluctuation spectrum, with a minimum amount of formal theoretical manipulation. We find that the decrease in the thermal conductivity produced by a finite frequency corresponds to an equivalent rise in temperature. This allows us to obtain the needed frequency dependence by using the temperature dependence measured by Ahlers[5] at zero frequency. The frequency-dependent relaxation rate found in this way is applied in Sec. IV to a detailed treatment of the fluctuation spectrum. Good comparison is found between the theory and the light scattering data, as illustrated in Fig. 7. Predictions are also made to further such experiments. Section V provides a brief summary.

It is perhaps useful, before embarking on the calculations, to reiterate that *it is not the purpose* of this paper *to provide a complete and detailed treatment of the critical dynamics of the λ transition* in liquid ^{4}He. Our goal is much more restricted and manageable: We want to demonstrate simply that the Ahlers experimental data contain all of the information required for understanding the light scattering data above the λ point. For the sake of simplicity and readability we include in this paper only the minimum amount of theory that is needed as a framework, or skeleton, on which to hang this demonstration. In other words, our paper can be regarded as a glimpse inside a "black box" which converts a certain "input" (experimental temperature dependence of the thermal conductivity) into an "output" (fluctuation spectrum). We call upon the theory only to the extent necessary to provide a working mechanism for this black box. Our aim, by establishing the connection between the two different experiments associated with the input and output, is to reduce the subsequent task of the theory to an account of the input alone. This latter task is the subject matter of another paper[14] and is not included here. We therefore ask the patient reader to accept the spirit and motivation of the "divide and conquer" tactic adopted here and not to insist on a full theoretical derivation of the input at this time.

II. CRITICAL THERMAL CONDUCTIVITY

The critical properties of liquid helium near the λ point are customarily described in terms of fluctuations in the complex Ginzburg-Landau field $\psi = |\psi| e^{i\phi}$, rather than in terms of the particle picture used in Sec. I. The Fourier coefficient of ψ expresses the number of helium atoms of momentum $\vec{p} = \hbar \vec{k}$ as

$$n_{\vec{p}} = |\psi_{\vec{k}}|^2 \ . \tag{2.1}$$

$2\pi\hbar$ is Planck's constant. The application of Eq. (2.1) to critical properties requires that $2\pi/k$, the wavelength corresponding to $\vec{p}$, be very much larger than the average interatomic spacing. A measure of the latter is $2r_s$, with r_s defined in terms of the atomic density n by

$$n = 3/4\pi r_s^3 \ . \tag{2.2}$$

At the temperature $T = T_\lambda = 2.173\ ^\circ\mathrm{K}$, $r_s = 2.2$ Å, increasing by about 7% high up on the λ line. The critical dynamic properties are associated with the thermodynamic fluctuations

$$\delta\mu = -s\,\delta T + n^{-1}\delta P \ . \tag{2.3}$$

These fluctuations of the chemical potential are produced by the fluctuations δT and δP in the temperature and pressure, respectively. At the low frequencies of interest in this paper, δP can be neglected. According to the time-dependent Schrödinger equation the time derivative of the phase of ψ is

$$\dot{\phi} = \frac{d\phi}{dt} = -\frac{1}{\hbar}\delta\mu \ . \tag{2.4}$$

As we are interested in the response of liquid helium to an applied thermal gradient, we can write

$$\delta\mu = \vec{r}\cdot\nabla\mu = -\vec{r}\cdot\vec{F} \ , \tag{2.5}$$

where $\vec{F} = -\nabla\mu$ is a constant vector force field, independent of the spatial coordinate $\vec{r}$. After the lapse of a short time Δt, Eqs. (2.4) and (2.5) produce the phase change

$$\Delta\phi(\vec{r}) = \hbar^{-1}\Delta t\,\vec{F}\cdot\vec{r} = \hbar^{-1}\Delta\vec{p}\cdot\vec{r} \ , \tag{2.6}$$

where $\Delta\vec{p} = \vec{F}\cdot\Delta\vec{t}$, or

$$\dot{\vec{p}} = \vec{F} \ . \tag{2.7}$$

Equation (2.7) is nothing other than the standard superfluid equation of motion applied to the fluctuations in the condensate wave function. It is now convenient to switch from wave-mechanical to classical particle language, and to regard Eq. (2.7) as simply Newton's second law describing the acceleration of helium atoms of momentum $\vec{p}$. By isotropy, the unperturbed equilibrium Bose-Einstein distribution of Eq. (2.1),

$$g(\epsilon) \equiv n_{\vec{p}} = \frac{1}{e^{\beta(\epsilon-\mu)} - 1} \ , \tag{2.8}$$

depends upon $\vec{p}$ only via the kinetic energy $\epsilon = p^2/2m$. As before, m is the atomic mass and $\beta = (k_B T)^{-1}$. Equation (2.8) takes into account the interactions of the helium atoms only through their effect on μ, and is equivalent to the usual Ornstein-Zernike approximation for liquid helium above the λ point. Close to the λ point, and in the critical range of small momenta, where both $|\mu|$ and ϵ are small, we have $\beta(\epsilon - \mu) \ll 1$, so that Eq. (2.8) becomes

$$g(\epsilon) \approx \frac{k_B T_\lambda}{\epsilon - \mu} \ . \tag{2.9}$$

Introducing the inverse correlation length κ by

$$\mu = -\frac{\hbar^2}{2m}\kappa^2 \tag{2.10}$$

brings Eq. (2.9) into the Ornstein-Zernike form

$$g(\epsilon) = \frac{2mk_BT_\lambda}{\hbar^2}\frac{1}{k^2+\kappa^2} \ . \tag{2.11}$$

The error in this approximation is known to be only a few percent because of the very small value of the critical exponent η.

The steady-state linearized Boltzmann equation in the relaxation time approximation[15] is

$$\vec{F}\cdot\vec{v}\,g'(\epsilon) = -2\gamma_\psi(k,\kappa)\Delta g(k,\kappa) \ , \tag{2.12}$$

where $\Delta g(\vec{k},\kappa)$ is the perturbation in the distribution function, $\vec{v}=\vec{p}/m$ is the particle velocity, and $(2\gamma_\psi)^{-1}$ is the particle mean relaxation time, arising from the random scattering processes. Solving Eq. (2.12) for Δg and substituting for $g'(\epsilon)$ from Eqs. (2.9) and (2.10) yields

$$\Delta g = \frac{\vec{F}\cdot\vec{v}}{2\gamma_\psi}\frac{k_BT_\lambda}{(\epsilon-\mu)^2} = \frac{4m^2k_BT_\lambda}{\hbar^4}\frac{\vec{F}\cdot\vec{v}}{(k^2+\kappa^2)^2}\frac{1}{2\gamma_\psi} \ . \tag{2.13}$$

The critical mass current density $\vec{J}_m^c$ is now found by multiplying Eq. (2.13) by $m\vec{v}$ and integrating over all momentum values. Taking $\vec{v}$ in the direction of $\vec{F}$ and noting from isotropy that the square of the component of $\vec{v}$ is equivalent to $v^2/3$, we obtain

$$\vec{J}_m^c = \frac{4}{3}\vec{F}\frac{k_BT_\lambda}{\hbar^2}\frac{m}{(2\pi)^3}\int\frac{d^3k}{(k^2+\kappa^2)^2}\frac{k^2}{2\gamma_\psi} \ . \tag{2.14}$$

We now invoke the basic feature of the two-fluid model—namely, the counterflow[16] of normal fluid that must take place, equal and opposite to Eq. (2.14), in order that no net mass flow occurs. This counterflow carries entropy at the rate of $s=k_B\bar{\sigma}$ per particle, and hence heat at the rate of $k_BT_\lambda\bar{\sigma}$ per helium atom. The density of heat current is consequently, as a result of the counterflow,

$$\vec{Q} = -k_BT_\lambda\bar{\sigma}m^{-1}\vec{J}_m^c \ . \tag{2.15}$$

The force $\vec{F}$ is given in terms of the applied temperature gradient by

$$\vec{F} = -\nabla\mu = k_B\bar{\sigma}\nabla T \ . \tag{2.16}$$

Substituting Eqs. (2.14) and (2.16) into Eq. (2.15) and identifying the thermal conductivity λ from

$$\vec{Q} = -\lambda\nabla T \ , \tag{2.17}$$

we find

$$\lambda = k_B\frac{4}{3}\left(\frac{k_BT_\lambda\bar{\sigma}}{\hbar}\right)^2\frac{1}{8\pi^3}\int\frac{d^3k}{(k^2+\kappa^2)^2}\frac{k^2}{2\gamma_\psi(k,\kappa)} \ . \tag{2.18}$$

III. FREQUENCY DEPENDENCE

A. Local limit

Equation (2.18) is easily generalized to the frequency, wave number, and temperature-dependent thermal conductivity $\lambda(\omega,k,\kappa)$. In the hydrodynamic limit, which occupies us mainly here, we drop the k dependence and write simply $\lambda(\omega,\kappa)$. The critical temperature dependence is expressed via κ. By including $\partial\Delta g/\partial t$ in Eq. (2.12) we find the response to an oscillatory but spatially uniform temperature gradient at angular velocity ω to be

$$\lambda(\omega,\kappa) = k_B\frac{4}{3}\frac{\gamma_0^2\bar{\sigma}^2}{8\pi^3}\int\frac{d^3k}{(k^2+\kappa^2)^2}\frac{k^2}{-i\omega+2\gamma_\psi(k,\kappa)} \ . \tag{3.1}$$

Here we have introduced

$$\gamma_0 = \frac{k_BT_\lambda}{\hbar} \tag{3.2}$$

to provide a characteristic frequency scale. A related constant of the liquid is the characteristic diffusion coefficient

$$D_0 = \frac{\hbar}{m} = 1.58\times10^{-4}\ \mathrm{cm^2/sec} \ . \tag{3.3}$$

The Bose-Einstein distribution gives a natural high momentum cutoff at an effective Debye wave number given by $\hbar^2k_D^2/2m = k_BT_\lambda$. Thus Eqs. (3.3) and (3.2) are related to one another by $\gamma_0 = \frac{1}{2}D_0k_D^2$. Alternatively we can obtain Eq. (3.3) from the standard kinetic theory formula v_l, where v is a mean velocity and l the mean free path of the helium atoms. (We omit the usual factor of $\frac{1}{3}$.) Taking $2\pi l$ equal to the De Broglie wavelength h/mv leads to Eq. (3.3).

Elsewhere[14] we have shown that Eq. (2.18) is in complete agreement with the Ahlers[5] data, both in absolute magnitude and in temperature dependence, provided account is properly taken of (i) transients and (ii) two-loop enhancement. (The latter effect corresponds to the phenomenon of "velocity persistence" in the language of kinetic theory.[17]) As explained at the end of Sec. I, we ask the indulgent reader to accept the Ahlers data as input and to follow us in seeing what a minimal black-box theory will then yield as an output, in the form of predicted fluctuation spectra for the light scattering experiment. We therefore turn now to the additional feature posessed, by Eq. (3.1), namely, its dependence upon $-i\omega$. We have already studied this question and have found[18] that the frequency dependence can be written as

$$\frac{\lambda(\omega,\kappa)}{\lambda(0,\kappa)} = \left(1-i\frac{\omega}{\sigma'}\right)^{-1/3} = (Z'/\sigma')^{-1/3} \ , \tag{3.4}$$

where

$$\sigma' = \frac{20}{21}\sqrt{\pi}\frac{\Gamma(\frac{1}{4})}{\Gamma(\frac{3}{4})} a_\psi \kappa^{3/2} = 5.0 a_\psi \kappa^{3/2} \tag{3.5}$$

and

$$Z' = \sigma' - i\omega \ . \tag{3.6}$$

The parameter σ' differs somewhat from the parameter σ of Eq. (20) of Ref. 18. But, like σ, σ' is proportional to $a_\psi \kappa^{3/2}$, the local (i.e., $k=0$) order-parameter relaxation rate. As $\lambda(0,\kappa) \propto \kappa^{-1/2} \propto \sigma'^{-1/3}$, it follows from Eq. (3.4) that $\lambda(\omega,\kappa)$ is obtained from $\lambda(0,\kappa)$ by replacing σ' by Z'. Therefore it is not necessary to regard $\lambda(\omega,\kappa)$ as a function of the two separate variables ω, κ. Instead, we change our notation to write $\lambda = \lambda(Z')$, a function of the single scaling variable Z'. As mentioned in Sec. I, this means that the frequency dependence is already fixed by the critical temperature dependence. We hasten to add, as noted in Ref. 18, that Eq. (3.4) is an approximation. The correction factor $F_S(Z_S)$, where Z_S is a certain scaled frequency, is plotted in Fig. 1. Although asymptotically $F_S \to 1.2$ as $Z_S \to \infty$, corresponding to the 20% underestimate mentioned in Ref. 18 for Eq. (3.4), the rise is very slow. In the frequency range of interest the error is less than 10%, and will be neglected here.

The zero-frequency Ahlers[5] data was found[14] to be represented by

$$\lambda = 21.6\left(\frac{c_P}{k_B}\right)^{1/2} t^{-1/3}(1 - 1.18t^{0.067} + 26.1t^{0.64}) \ , \tag{3.7}$$

in the units of μW/°K cm. The second and third terms within the parentheses are the slow and fast transients, respectively. As mentioned above, the slow transient enters with negative amplitude. We have noted[14] that this minus sign is essential for producing the stronger divergence found by Ahlers.[5] For the present purposes, Eq. (3.7) can be regarded as an empirical fit which serves as a convenient way

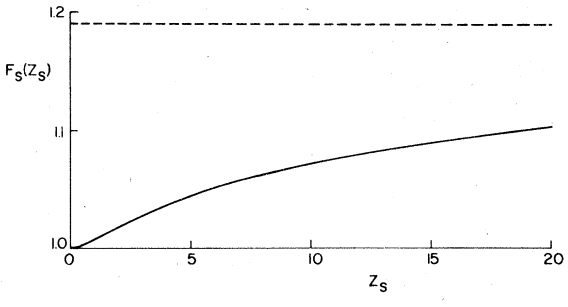

FIG. 1. Entropy relaxation rate scaling function $F_S(Z_S)$ vs Z_S. The dashed line represents the asymptotic value of 1.19. F_S changes by less than 10% in the Z_S range of interest.

of describing the input, in the sense of Sec. I. The fact that the numerical values of the transient exponents inside the parentheses and of the scaling coefficient in front are predicted by the underlying theory is not relevant for the present black-box approach to the fluctuation spectrum. The only thing that we require for this approach is an extension of Eq. (3.7) to nonzero frequencies. This is provided by the above scaling considerations,[19] which permit us to replace the zero-frequency temperature parameter σ' by the combined frequency-temperature scaling variable Z'. With

$$\kappa = \kappa_0 t^{2/3} \tag{3.8}$$

and $\kappa_0 = 0.7$ Å^{-1}, we can express the temperature dependence in Eq. (3.7) entirely in terms of κ. Dividing by the specific heat gives the thermal diffusion coefficient, again as a function of κ. Equation (3.5) then permits κ to be replaced by σ', which in turn is replaced by Z'. Dividing by the specific heat then yields a "universal" critical entropy diffusion coefficient $D_S(Z')$, containing both the temperature and frequency dependence. $D_S(Z')$ takes on the background value $B_S = 2.0 \times 10^{-4}$ cm^2/sec as Z' becomes large. The entropy relaxation rate γ_S is obtained by multiplying by the square of $k = 1.79 \times 10^5$ cm^{-1}, the wave number in the Tarvin *et al.*[6] experiment. Comparison with Eq. (3.3) shows that $B_S \approx D_0$, as expected *a priori*.

It is convenient to redefine the scaling variable Z' in the dimensionless form

$$Z = Z'/a_\psi k^{3/2} = \tilde{\sigma} - i\tilde{\Omega} \ , \tag{3.9}$$

where

$$\tilde{\Omega} = \omega/a_\psi k^{3/2} \tag{3.10}$$

and

$$\tilde{\sigma} = 5.0\left(\frac{\kappa}{k}\right)^{3/2} \ , \tag{3.11}$$

differing from the corresponding variables Ω and σ of Ref. 18 by the factor σ_ψ^{-1} (i.e., $\tilde{\sigma} = \sigma/\sigma_\psi$). $\omega_\psi = a_\psi k^{3/2}$ is the scaling value of the order-parameter relaxation rate at $\kappa = 0$. (Its numerical value is $\omega_\psi/2\pi = 0.6$ MHz for $k = 1.79 \times 10^5$ cm^{-1}.) From the above equations we find, in units of MHz,

$$\frac{D_S k^2}{2\pi} = \frac{\gamma_S}{2\pi} = \frac{10.35}{Z^{1/3}}\left(\frac{k_B}{c_P}\right)^{1/2}(1 - 0.582Z^{0.067} + 0.0234Z^{0.64}) \ , \tag{3.12}$$

where c_P is the specific heat per particle, in units of k_B. Over the intermediate range of Z values c_P can be fitted sufficiently accurately by a power law, which

puts Eq. (3.12) into the convenient form

$$\frac{\gamma_S}{2\pi} = \frac{5.192}{Z^{0.263}} - \frac{3.022}{Z^{0.196}} + 0.122 Z^{0.381} , \qquad (3.13)$$

again in MHz. The background value of B_S mentioned above leads to a background for $\gamma_S/2\pi$ of $B_S k^2/2\pi = 1.0$ Mhz. This has been subtracted from $\gamma_S/2\pi$ and the remaining critical portion plotted in Fig. 2 versus Z. γ_S drops rapidly with increasing Z. This can result from a rise in temperature, from a change in the frequency variable, or from finite resolution. It will be noted that, except for relatively small values of Z, the critical portion of $\gamma_S/2\pi$ is smaller than its background portion. Furthermore, this range for Z is effectively inaccessible in the experiment of Tarvin, Vidal, and Greytak.[6] This is because, as explained in Sec. IV, convolving the experimental resolution function adds Γ_0/ω_ψ to Z (where Γ_0 is the half-width at half maximum). With $\Gamma_0/2\pi = 1.5$ MHz, this addition becomes 2.5, as indicated by the left-hand vertical dashed line in Fig. 2. Only the portion of the curve to the right of the dashed line is observable in experiments with this resolution. It is therefore evident that the critical portion of $\gamma_S/2\pi$ contributing to the light scattering

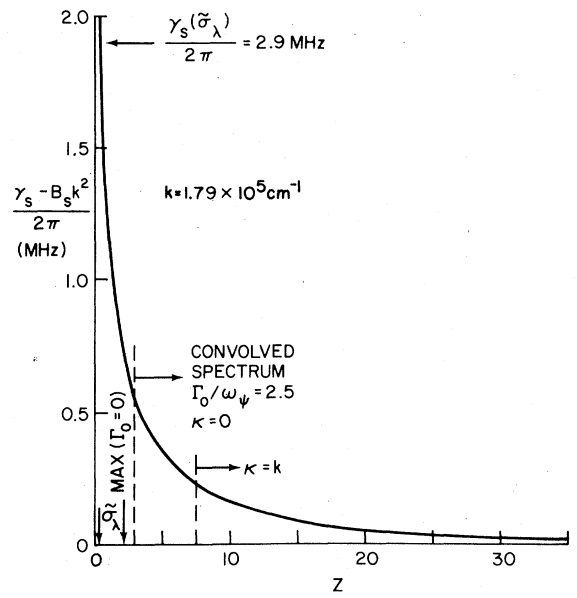

FIG. 2. Entropy relaxation rate γ_S (with the background of 1.0 MHz subtracted) vs the scaling variable Z. $\tilde{\sigma}_\lambda = 0.41$ is the limiting value of $\tilde{\sigma}$ as $T \to T_\lambda$. MAX($\Gamma_0 = 0$) corresponds to the frequency at the maximum in the infinite resolution λ-point spectrum. The dashed lines are drawn for the two different temperatures for which $\kappa = 0$ and $\kappa = k$ and correspond to the Tarvin *et al.* (Ref. 6) resolution. The portion of the curve to the right of this line determines the spectrum.

spectrum is never larger than 50% of the background value. This explains qualitatively the relative lack of temperature variation in the spectrum for $T \geqslant T_\lambda$, with this question handled quantitatively in Sec. IV. For $T > T_\lambda$ the minimum value of Z is $\Gamma_0/\omega_\psi + \tilde{\sigma}$. $\tilde{\sigma}$ increases linearly with $T - T_\lambda$, which further restricts the range of Z which is involved in the light scattering spectrum. The second dashed line in Fig. 2 illustrates the shift to the right and the lessening of critical behavior for the temperature at which the correlation length equals $(2\pi)^{-1}$ times the scattering wavelength (i.e., $\kappa = k$). In each of these cases the structure of γ_S to the left of the dashed line is inaccessible to observation. As the sharpest structure occurs at the smalles values of Z, it is clear why even a small value of Γ_0 or a moderate increase in temperature can have a big effect in washing out the spectrum. A rise in temperature moves the accessible range of Z to the right, causing a loss of structure, with the spectrum soon becoming Lorentzian.

B. λ-point nonlocality

As shown in Sec. IV, the above treatment of γ_S is quite adequate for giving a full account of the fluctuation spectra as observed with the presently attainable experimental resolution. It is, however, based on the $k = 0$ local approximation and neglects the k dependence of $\lambda(\omega, k, \kappa)$. In this approximation the $\omega = 0$ value of γ_S continues to increase as $T \to T_\lambda$ and becomes infinite at the λ point. Consequently the resulting entropy fluctuation spectrum vanishes at $\omega = 0$, as shown in Fig. 12 of Ref. 12. But because of the finite value of k, $\gamma_S(0, k, 0) < \infty$, and the spectrum does not in fact vanish as $\omega = 0$. It will look more like the two lower curves in Fig. 1 of Ref. 18 (for $\sigma^{1/3} = \frac{1}{8}$ and $\frac{1}{2}$), rather than the extreme case of Ref. 12. Because of the experimental resolution, the central valley of the spectrum is not observable in any case, and the error produced by the $k = 0$ local approximation has only an imperceptible effect on the convolved spectrum. Nevertheless, we include here a brief treatment of the nonlocal correction that is required close to and at the λ point. The reader who is primarily interested in how the experimental spectra compare with the theoretical predictions does not need this nonlocal refinement. He may wish to skip the remainder of this section and go directly to Sec. IV.

The full ω, k, and κ dependence of γ_S has been calculated by Dohm[13] in the ϵ expansion. We restrict ourselves here to the $\omega = 0$ limit. All of the k and κ dependence is then contained in the scaling function

$$H(k, \kappa) = \tfrac{1}{2} \ln(\kappa^2 + \tfrac{1}{4} k^2) - 2 \frac{\kappa^2}{k^2} \ln \frac{\kappa^2}{\kappa^2 + \frac{1}{4} k^2} - \tfrac{1}{2} , \qquad (3.14)$$

which in the $k \to 0$ limit is simply $\ln\kappa$, the local approximation. The first term of the right-hand member of Eq. (3.14) puts κ on a par with $\frac{1}{2}k$, and is consistent with the rough rule of thumb.[20] This is modified by the last two terms, which equal 0 and $-\frac{1}{2}$ for $k=0$ and $\kappa=0$, respectively. Consequently the $\kappa=0$ limit can be expressed by

$$H(k,0)=H(0,\kappa_{\text{eff}}) \ , \tag{3.15}$$

where $\kappa_{\text{eff}}=k/2\sqrt{e}=k/3.3$.

The factor of $l=3.3$ found above corresponds to the so-called "threshold factor" in the dispersion theory approach.[21] In the field theory analogue l describes the effective number of intermediate-state particles involved in a particular many-body process. In Ref. 12 we found that the two-term ϵ expansion was not sufficiently accurate for estimating integrals in three dimensions (i.e., for $\epsilon=1$). Better accuracy is obtained with the so-called "$\bar{\epsilon}$-expansion," which in Appendix A yields the preferred value of $l=5.0$. Substituted into Eq. (3.11) this gives

$$\tilde{\sigma}_\lambda=5.0\left(\frac{\kappa_{\text{eff}}}{k}\right)^{3/2}=5.0l^{-3/2}=5.0^{-1/2}=0.41 \ . \tag{3.16}$$

Using $\tilde{\sigma}_\lambda$ in the local expression for γ_S at the λ point, rather than $\tilde{\sigma}=0$, effectively introduces the required correction for the nonlocality. $\tilde{\sigma}_\lambda$ is indicated by the downwards pointing arrow in the lower left-hand corner of Fig. 2. The corresponding value $\gamma_S(\tilde{\sigma}_\lambda)/2\pi=2.9$ MHz is indicated by the horizontal arrow at the top of Fig. 2.

At this point the critical reader will detect an inconsistency. Following Ref. 18 [see, especially, Eqs. (19) and (20)], we have defined $\tilde{\sigma}$ in Sec. III A above [Eqs. (3.5), (3.6, (3.9), and (3.11)] in terms of the frequency scale. This is accomplished by equating $3\sigma'$ to the reciprocal of the logarithmic frequency derivative of γ_S. Equation (3.16) on the other hand, fixes $\tilde{\sigma}_\lambda$ only from the zero-frequency value of γ_S, with no reference to its frequency derivative. This is because at the λ point, the Ahlers[5] $k=0$ thermal conductivity data are not directly applicable. Therefore, we need to extract not one, but *two* pieces of information from the theory. The situation is different from that in the $T > T_\lambda$ local limit, where the value of γ_S is already known from the Ahlers data and we only need from the theory information on the frequency derivative. We have followed the alternative approach to determining $\tilde{\sigma}_\lambda$ from the frequency scale at the λ point and have found a value approximately twice that of Eq. (3.16). The inconsistency results from the error in forcing the frequency dependence of γ_S to conform to the simple one-parameter treatment based on Eq. (3.6). As reported following Eq. (21) of Ref. 18, this approach underestimates $\gamma(0,k,0)$, which is correctly rendered only by the smaller value of $\tilde{\sigma}_\lambda$. The spectrum based on the single-parameter approach with $\tilde{\sigma}_\lambda=0.41$ is discussed in Sec. IV (see Fig. 5, below). A more accurate two-parameter spectrum which takes into account the larger $\tilde{\sigma}_\lambda$ correctly describing the frequency scale has also been calculated. But not being significantly different, it is not exhibited in this paper. The improved two-parameter spectrum is slightly broader with a somewhat reduced peak-to-valley ratio (decreased by approximately 20%).

IV. FLUCTUATION SPECTRUM

In this section we study the fluctuation spectrum arising from the temperature and frequency-dependent entropy self-energy γ_S and thereby make contact with the light scattering experiments of Tarvin, Vidal, and Greytak.[6] The observed spectral intensity versus frequency at given κ for infinite resolution is the real part of the entropy Green's function

$$G_S=\frac{1}{-i\omega+\gamma_S(\omega,\kappa)} \tag{4.1}$$

provided $\kappa \gg k$. In general, every instrument has its own resolution function $L(\omega)$ and the fluctuation spectrum actually observed is therefore

$$\begin{aligned}\text{Re}g_S(\omega)&=\int_{-\infty}^{\infty}\text{Re}G_S(\omega-\omega')L(\omega')\,d\omega' \\ &=\text{Re}\int_{-\infty}^{\infty}G_S(\omega-\omega')L(\omega')\,d\omega' \ .\end{aligned} \tag{4.2}$$

The second line follows from the reality of $L(\omega')$.

One of the simplest forms for the resolution function is the Lorentzian

$$L_1(\omega)=\frac{1}{\pi}\frac{\Gamma_0}{\omega^2+\Gamma_0^2} \ , \tag{4.3}$$

normalized to $\int_{-\infty}^{+\infty}L_1(\omega)\,d\omega=1$. $L_1(\omega)$ is shown in Fig. 3 by the curve labeled "LOR." The frequency unit has been chosen $\Gamma_0=1$. In the experiments of

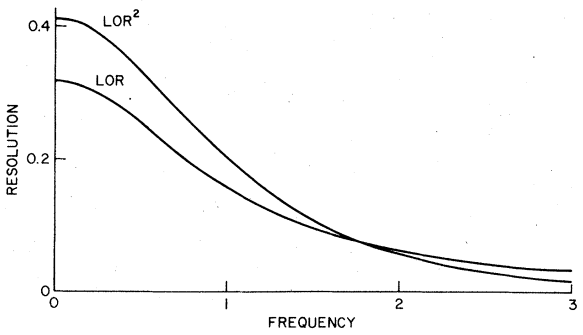

FIG. 3. Resolution function vs frequency. The curve labeled LOR is a Lorentizan with unit half-width and unit area. The curve identified by LOR^2 is a squared Lorentzian with the same half-width and normalization.

Tarvin *et al.*[6] the resolution function has, however, a weaker tail than the Lorentzian, and is better approximated by

$$L_2(\omega) = \frac{1}{\pi} \frac{2\Gamma_1^3}{(\Gamma_1^2 + \omega^2)^2} \tag{4.4}$$

shown in Fig. 3 by the curve labeled LOR^2. The area has once again been normalized to unity and this function has the same half-width as $L_1(\omega)$, provided

$$\Gamma_1 = (1+\sqrt{2})^{1/2}\Gamma_0 \ . \tag{4.5}$$

It is evident from the figure that L_2 has a weaker tail than L_1. To conserve the area it has to be stronger at the center.

We now carry out the convolution indicated in Eq. (4.2) with the functions $L_1(\omega)$ and $L_2(\omega)$. The integration can be done easily using the Cauchy residue theorem. For $L_1(\omega)$ the convolution integral becomes

$$\mathrm{Re}g_S(\omega) = \mathrm{Re}G_S(\omega + i\Gamma_0) \ , \tag{4.6}$$

while for $L_2(\omega)$ it is

$$\mathrm{Re}g_S(\omega) = \mathrm{Re}G_S(\omega + i\Gamma_1) + \Gamma_1 \mathrm{Im}G_S'(\omega + i\Gamma_1) \ . \tag{4.7}$$

The prime denotes differentiation with respect to ω. To demonstrate the differing effects of $L_1(\omega)$ and $L_2(\omega)$ on the true unconvolved spectrum $G_S(\omega)$, we consider a case in which $G_S(\omega)$ has a particularly simple form. This is the case for $T = T_\lambda$ and $w = 0$. We have established earlier[18] that for this case

$$\omega_c G_S(\omega) = \frac{1}{-i\omega/\omega_c + (-i\omega/\omega_c)^{-1/3}} \ , \tag{4.8}$$

where we are using the notation of Ref. 18. This unconvoluted spectrum is identified by the label $\Gamma_0 = 0$ in Fig. 4 and has the deep valley and sharp peak described in our earlier work. The effect of smearing it out according to Eq. (4.6) with a Lorentzian resolution function having $\Gamma_0 = 1$ is shown in Fig. 4 by the curve labeled LOR. We see that the structure has disappeared and that the spectrum has acquired a half-width of 2.25, in units of ω/ω_c. The curve labeled LOR^2 in Fig. 4 exhibits the effect of convolving with $L_2(\omega)$ for $\Gamma_1 = (1+\sqrt{2})^{1/2} = 1.55$. The structure remains washed out, although the half-width has been reduced to 2.07, in units of ω/ω_c. This decrease by 9% results from the relatively more compact form of L_2.

The above $w = 0$ spectrum, although serving to illustrate the effect of instrumental resolution, does not give a realistic picture of the true λ-point spectrum at infinite resolution. As explained at the end of Sec. III, a sufficiently accurate λ-point spectrum is obtained from the "universal" self-energy function γ_S of Fig. 2 by setting $\tilde{\sigma}$ equal to a $T \to T_\lambda$ limiting value, $\tilde{\sigma}_\lambda$, which we estimated at 0.41. Inserting this value of $\tilde{\sigma}$ into Eq. (3.13) gives the λ point γ_S as a function of frequency. Substituting this γ_S into Eq. (4.1), measuring frequency in units of ω_ψ, and taking the real part, gives us the $\Gamma_0 = 0$ curve of Fig. 5. As discussed in Sec. III, which should be referred to for additional critical comments, this curve is at present only of theoretical interest because of the limited experimental resolution. It is included only for the sake of completeness. We emphasize that for the purpose of comparing with the light scattering data that presently exist, we can set $\tilde{\sigma}_\lambda = 0$ and neglect the nonlocality of the critical thermal conductivity.

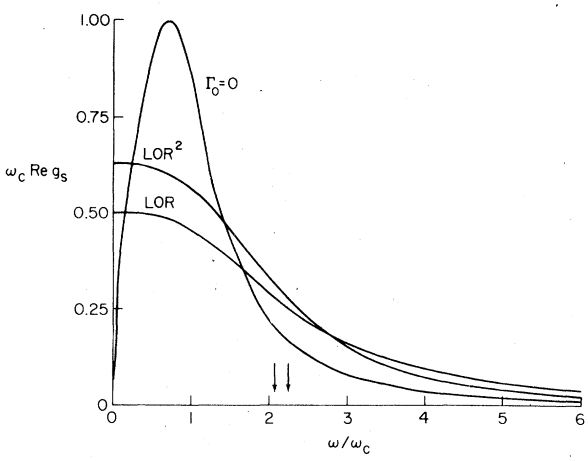

FIG. 4. Idealized λ-point spectrum for $w = 0$ vs dimensionless frequency. The curve labeled $\Gamma_0 = 0$ is the infinite resolution spectrum. Convolving with a Lorentzian and with a squared Lorentzian gives the curves labeled LOR, and LOR^2, respectively. The half-widths differ by 9%, as indicated by the vertical arrows.

The λ-point spectrum that we find from the above procedure still has a pronounced structure, although somewhat milder than in the $w = 0$ case. The structure disappears when we fold in the experimental

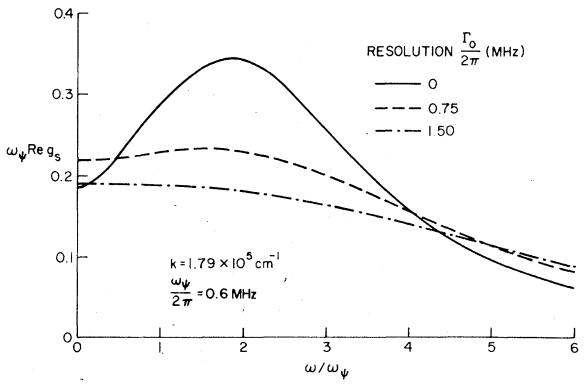

FIG. 5. Predicted λ-point spectrum vs dimensionless frequency for wave number $k = 1.79 \times 10^5\ \mathrm{cm}^{-1}$, convolved with Lorentzian resolution functions for the three different resolutions shown.

resolution of $\Gamma_0/2\pi = 1.5$ MHz, treating the resolution function as a Lorentzian, for simplicity. The dot-dash curve of Fig. 5 represents this case. The half-width is 3.4 MHz, or 5.7 in units of ω_ψ. Of the various spectra exhibited by Tarvin *et al.*,[6] the $q\xi = 21$ spectrum is the one closest to the λ point. The half-width of this spectrum is evidently 3.1 MHz, about 10% smaller than ours. But we have seen earlier that using a more realistic resolution function can decrease the half-width by approximately this amount. Thus the experiment and the present theory are in good agreement regarding the absolute scale of the spectral width. The remaining graph—the dashed curve—in Fig. 6 represents the case where the resoltuion is improved by a factor of 2. It can be seen that a faint hint of structure reappears. The underlying structure still remains largely washed out.

Tarvin, Vidal, and Greytak[6] fitted their spectra at different temperatures to double-Lorentzian shapes and reported the results of their measurements in the form of the two fitting parameters ω_2 (frequency shift) and Γ_2 (damping) as a function of temperature. Consequently we fit our predicted spectra in the same way and thereby predict the temperature dependences of ω_2 and Γ_2. In doing the convolutions, we use a Lorentzian resolution function, $L_1(\omega)$. This approximation should not seriously impair our determination of ω_2 and Γ_2, as L_1 will be convolved with *both* the theoretical spectrum and the double Lorentzian. Any inadequacies of L_1 can be expected to drop out in the comparison. The double Lorentzian is the real part of

$$G_2(\omega) = \frac{1}{2}\left[\frac{1}{-i(\omega-\omega_2)+\Gamma_2} + \frac{1}{-i(\omega+\omega_2)+\Gamma_2}\right] . \tag{4.9}$$

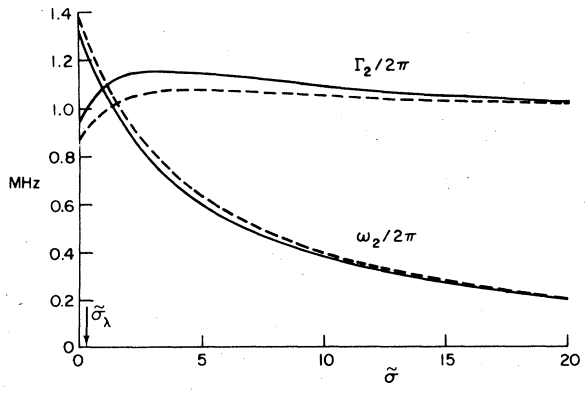

FIG. 6. Double-Lorentzian parameters Γ_2 and ω_2 vs the temperature parameter σ. The dashed curves follow from Eqs. (4.12) and (4.16), while the solid curves resulting from the matching of the central value and curvature of the spectrum follow from Eqs. (4.12) and (4.17).

Convolved with $L_1(\omega)$, this becomes

$$g_2(\omega) = \frac{1}{2}\left[\frac{1}{-i(\omega-\omega_2)+\Gamma_2+\Gamma_0} + \frac{1}{-i(\omega+\omega_2)+\Gamma_2+\Gamma_0}\right] . \tag{4.10}$$

This is to be compared with the theoretical spectrum from Eqs. (4.1) and (4.6),

$$g_S(\omega) = \frac{1}{-i\omega+\Gamma_0+\gamma_S(\omega+i\Gamma_0)} . \tag{4.11}$$

The two parameters ω_2 and Γ_2 can now be determined by matching two features of the two equations (4.10) and (4.11). The first one is the strength at the center, i.e., the $\omega = 0$ value. This yields

$$\Gamma_0 + \gamma_S(i\Gamma_0) = \frac{(\Gamma_2+\Gamma_0)^2+\omega_2^2}{\Gamma_2+\Gamma_0} = \Gamma_2+\Gamma_0+\frac{\omega_2^2}{\Gamma_2+\Gamma_0} , \tag{4.12}$$

or

$$\gamma_S(i\Gamma_0) = \Gamma_2 + \frac{\omega_2^2}{\Gamma_2+\Gamma_0} .$$

In order to impose a second condition on the two spectral parameters Γ_2 and ω_2, it is convenient to define an effective self-energy for $g_2(\omega)$ according to

$$g_2(\omega)^{-1} = -i\omega + \gamma_{\text{eff}} . \tag{4.13}$$

Substituting Eq. (4.10) into Eq. (4.13) we find

$$\gamma_{\text{eff}}(iz) = \Gamma_2 + \frac{\omega_2^2}{z+\Gamma_2} , \tag{4.14}$$

where $z = -i\omega$. Note that $\gamma_{\text{eff}}(i\Gamma_0) = \gamma_S(i\Gamma_0)$ by Eq. (4.12). We now obtain the needed second condition by requiring that the first derivatives should also agree. Namely,

$$\left.\frac{d\gamma_S}{dz}\right|_{\Gamma_0} = \left.\frac{d\gamma_{\text{eff}}}{dz}\right|_{\Gamma_0} = -\frac{\omega_2^2}{(\Gamma_0+\Gamma_2)^2} = \frac{\Gamma_2-\gamma_S(i\Gamma_0)}{\Gamma_2+\Gamma_0} , \tag{4.15}$$

where in the last step Eq. (4.12) has been used. Equation (4.15) can be written

$$\Gamma_2 = \frac{\gamma_S + \Gamma_0 d\gamma_S/dz}{1 - d\gamma_S/dz} ; \tag{4.16}$$

$\gamma_S(iz)$ and its derivatives are evaluated at $z = \Gamma_0$. Equation (4.16), together with Eq. (4.12) fixes the parameters Γ_2 and ω_2.

The condition expressed by Eq. (4.16) was obtained by going perpendicular to the real frequency axis. The true physical frequency dependence occurs, of course, parallel to the real axis. Therefore we

have developed an alternative matching procedure which fits the central curvature of the double Lorentzian to the zero-frequency curvature of the theoretical spectrum. The details are provided in Appendix B. Here we simply quote the final result:

$$\frac{1}{\Gamma_0+\Gamma_2}=\frac{1}{\Gamma_0+\gamma_S}-\frac{1}{3}\frac{1}{\Gamma_0+\gamma_S}\left[2\frac{d\gamma_S}{dz}+\left[\frac{d\gamma_S}{dz}\right]^2\right]+\frac{1}{6}\frac{d^2\gamma_S}{dz^2}\ . \tag{4.17}$$

Again, $\gamma_S(iz)$ and its derivatives are evaluated at $z=\Gamma_0$. The parameters Γ_2 and ω_2 are obtained as functions of the "temperature variable" $\tilde{\sigma}$ and plotted in Fig. 6. The dashed curves are the results of using Eqs. (4.16) and (4.12), while the solid curves follow from Eqs. (4.17) and (4.12). The qualitative features of both curves are similar. For $\tilde{\sigma} >> 1$ (i.e., temperatures well removed from T_λ), Γ_2 is nearly flat, because of the constant thermal-conductivity background. In this limit $\omega_2 \approx 0$, as the spectrum is nearly Lorentzian. As we move closer towards the λ point, structure develops and ω_2 grows. This anticipates the separation into the second-sound doublet below T_λ. Because of the strong temperature dependence of γ_S, some variation in Γ_2 might also be expected. In fact, Γ_2 remains remarkably constant in the entire region $T > T_\lambda$, as seen in Fig. 6. This can be understood most easily from Eq. (4.16) where the increase of $\gamma_S(i\Gamma_0)$ in the numerator is largely canceled by the variation of the derivative. The relatively small difference between the solid and dashed curves of Fig. 6, obtained from two different computational methods, lends some confidence in the accuracy of these predictions. According to Eq. (3.11), $\tilde{\sigma} \to 0$ as the λ point is approached, provided nonlocality is neglected. The smallness of the error incurred in this approximation is indicated by the downwards pointing arrow in Fig. 6, located very near to the origin.

Figure 7 shows the comparison of our predicted temperature-dependent Γ_2 with the experimental Γ_2 data points. The solid and dot-dashed curves correspond to Eqs. (4.17) and (4.16), respectively. The dashed curve is the prediction of the planar spin model calculation of Hohenberg, Siggia, and Halperin (HSH).[22] The reason why their curve falls off so rapidly lies in their neglecting the fairly strong thermal-conductivity background, as well as their use of too large a value of w. Theirs is the standard dynamic scaling prediction, which would lead to a vanishing half-width at large values of κ. For comparison, the dotted curve shows the first "improvement" in the HSH curve that is provided by our theory. This results from the smaller value of w, but with the last two terms of Eq. (3.13) omitted. Dropping these transient terms serves to remove completely the effects of background. It is thereby evident that the second improvement, namely, the inclusion of background effects, is essential for bringing the theoretical prediction down to the solid curve and into agreement with experiment. Tarvin *et al.*[6] have not reported quantitatively the temperature dependence of ω_2 above T_λ. But from their Fig. 12 we conclude that at T_λ, $\omega_2/2\kappa = 1.3$ MHz. Our prediction (solid curve in Fig. 6) of $\omega_2/2\kappa = 1.34$ MHz is in good agreement.

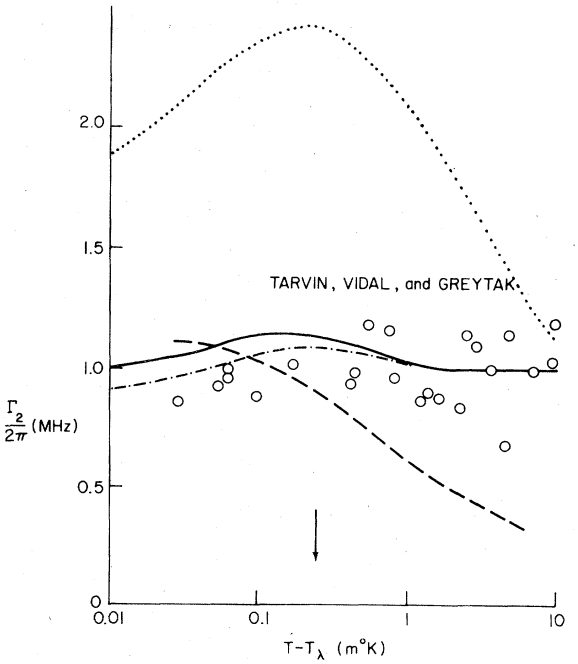

FIG. 7. Comparison of theoretical predictions with experimental data (circles) for Γ_2 vs temperature. The dashed curve shows conventional theory while the present calculations including background and frequency dependence are represented by the solid and dot-dash curves. The dotted curve shows the present theory without the transients (background terms). The arrow indicates the temperature at which $\kappa = k$.

As a final point we exhibit the effect of using light of shorter wavelength. We predict the λ-point spectra shown in Fig. 8 for the three different resolutions $\Gamma_0 = 0$, 0.75, and 1.5 MHz, with $k = 3.58 \times 10^5$ cm^{-1}. This is double the wave number previously employed by Tarvin *et al.*[6] A larger k immediately raises the value of σ_λ and consequently the $\Gamma_0 = 0$ spectrum becomes more filled in. (Compare the $\Gamma_0 = 0$ curves in Figs. 8 and 5.) Finite resolution washes out the remaining structure. We thus conclude that doubling the light frequency would not be helpful in observing structure in the spectrum. But it can serve a very important purpose. If the present considerations are correct, then experiments at this higher frequency should again produce a flat Γ_2 for $\kappa >> k$, and this

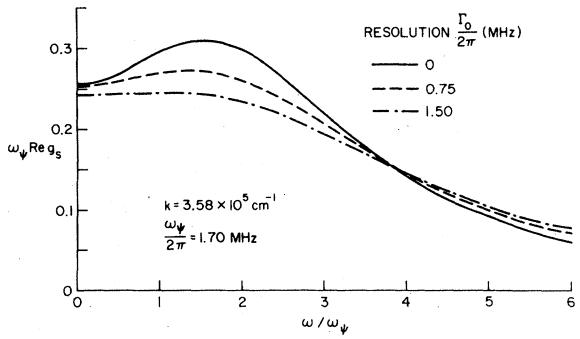

FIG. 8. Predicted λ-point spectrum vs dimensionless frequency for wave number $k = 3.58 \times 10^5\ \mathrm{cm}^{-1}$, convolved with Lorentzian resolution functions for the three different resolutions shown.

temperature-independent value should be *four times* the present value of 1 MHz. This predicted increase of Γ_2 is a factor of $\sqrt{2}$ times that predicted by dynamic scaling, or 41% bigger.

V. SUMMARY

From elementary kinetic theory using the linearized Boltzmann equation, a formula for the critical part of the thermal conductivity has been obtained which is identical to that derived in mode-coupling theory (for the local limit). A "universal" scaling variable Z is introduced which puts frequency and temperature changes on the same footing. This serves to eliminate, as a separate problem, the frequency dependence involved in the fluctuations that cause the light scattering. The frequency dependence instead gets reexpressed in terms of an equivalent temperature dependence of the zero-frequency thermal conductivity of liquid helium. The light scattering can therefore be predicted on the basis of the experimental measurements by Ahlers[5] of the static thermal conductivity. The detailed analysis of this equivalence has been expressed in terms of the dependence of the entropy relaxation rate γ_S on the scaling variable Z.

In Sec. IV, $\gamma_S(Z)$ has been used to study the fluctuation spectrum. The effect of a finite instrumental resolution has been considered and the λ-point spectra for different resolutions and optical wavelengths calculated. The calculated spectra were reported in terms of a two-parameter double-Lorentzian representation and the two parameters Γ_2 and ω_2 exhibited as functions of temperature. The comparison of these results with the findings of Tarvin, Vidal, and Greytak[6] was quite satisfactory. Although this paper has been limited to $T \geq T_\lambda$, we have also studied the $T \leq T_\lambda$ region[14] and have concluded that also there the light scattering observations can be largely accounted for.

ACKNOWLEDGMENTS

We are glad to acknowledge stimulating discussions with Professor T. Greytak, as well as support from the NSF under Grants No. DMR-76-24472, No. DMR-76-82345, and No. DMR-76-81185.

APPENDIX A: THRESHOLD FACTOR

In Sec. III we found an approximate value for the threshold factor $l = k/\kappa_{\mathrm{eff}}$ from Dohm's[13] ϵ expansion of the scaling function. Improved accuracy for $\epsilon = 1$ can be obtained by instead using the $\bar{\epsilon}$ approximation of Ref. 12. The zero-frequency thermal conductivity is proportional to the scaling function

$$\Lambda(k,\kappa) = \frac{1}{4\pi k^2} \int \frac{d^3p\,(p^2 - p'^2)^2}{(p^2+\kappa^2)(p'^2+\kappa^2)} \frac{1}{\gamma(p)+\gamma(p')} , \tag{A1}$$

where

$$\gamma(p) = (p^2+\kappa^2)^{3/4} \tag{A2}$$

and

$$\vec{p} + \vec{p}\,' = \vec{k} . \tag{A3}$$

The $k \neq 0$ nonlocal effects fall outside the simple kinetic theory framework of Secs. II and III of this paper, and have to be derived as in Ref. 12 by mode coupling or by some equivalent formalism. We are interested in the extreme local limit

$$\Lambda(0,\kappa) = J_{\mathrm{L}} \kappa^{-1/2} \tag{A4}$$

and in the extreme nonlocal limit

$$\Lambda(k,0) = J_{\mathrm{NL}} k^{-1/2} , \tag{A5}$$

where

$$J_{\mathrm{L}} = \tfrac{2}{3} \int_0^\infty \frac{d\pi}{(\pi^2+1)^{3/4}} \left(\frac{\pi^2}{\pi^2+1} \right)^2 \tag{A6}$$

and

$$J_{\mathrm{NL}} = \frac{1}{4\pi} \int \frac{d^3p\,(p^2-p'^2)^2}{p^2 p'^2 (p^{3/2}+p'^{3/2})} . \tag{A7}$$

In Eq. (A7) the momenta have been scaled to $k = 1$. Proceeding as at the end of Sec. III, we define the threshold factor by

$$\Lambda(0,\kappa_{\mathrm{eff}}) = \Lambda(0,k/l) = \Lambda(k,0) . \tag{A8}$$

Substituting Eqs. (A4) and (A5) gives

$$l = \left(\frac{J_{\mathrm{NL}}}{J_{\mathrm{L}}} \right)^2 . \tag{A9}$$

For the local case the integration can be carried out

exactly and yields

$$J_{\mathrm{L}}=\tfrac{1}{3}\beta(\tfrac{5}{2},\tfrac{1}{4})=1.00\ . \tag{A10}$$

The nonlocal case is more difficult and requires an approximate evaluation. By means of the techniques of Appendix B of Ref. 12 we find the two-term $\bar{\epsilon}$ expansion

$$J_{\mathrm{NL}}=\frac{2}{3}\frac{1}{\bar{\epsilon}}\bigg|_{\bar{\epsilon}=1/2}+\tfrac{8}{9}=\tfrac{20}{9}=2.22\ . \tag{A11}$$

(The integral is the same as evaluated there, except for the absence of the finite frequency term in the denominator, and again is rendered with better than 1% accuracy.) Substituting Eqs. (A10) and (A11) into Eq. (A9) yields $l=5.0$, as reported in Sec. III. This value is used instead of the ϵ-expansion value of 3.3.

APPENDIX B: ALTERNATIVE MATCHING CONDITION

The parameter Γ_2 of the double Lorentzian equivalent to the theoretically predicted spectrum was calculated in Sec. IV from the behavior of an effective self-energy along the imaginary frequency axis. In this Appendix we impose instead a condition on the real spectrum and calculate the resulting Γ_2. The condition consists of adjusting Γ_2 and ω_2 so as to match the central (i.e., $\omega=0$) curvature of the double Lorentzian with that of the theoretical spectrum.

The easiest way to extract the central curvature is to Taylor-expand the real part of the Green's function about $\omega=0$ and look for the coefficient of the ω^2 term. Working to $O(\omega^2)$, we first need

$$\gamma_S(\omega+i\Gamma_0)=\gamma_S+(-i\omega)\frac{d\gamma_S}{dz}+\frac{(-i\omega)^2}{2!}\frac{d^2\gamma_S}{dz^2}\ , \tag{B1}$$

where $z=-i\omega$ and γ_S and its derivatives are evaluated at $z=\Gamma_0$. Thus,

$$g_S(\omega+i\Gamma_0)=\frac{1}{-i\omega+\Gamma_0+\gamma_S(\omega+i\Gamma_0)}=\frac{1}{-i\left(\omega+\omega\dfrac{d\gamma_S}{dz}\right)+\gamma_S+\Gamma_0-\dfrac{\omega^2}{2}\dfrac{d^2\gamma_S}{dz^2}}\ , \tag{B2}$$

giving

$$\mathrm{Re}g_S(\omega+i\Gamma_0)=\left[\gamma_S+\Gamma_0-\frac{\omega^2}{2}\frac{d^2\gamma_S}{dz^2}+\frac{\omega^2(1+d\gamma_s/dz)^2}{\gamma_S+\Gamma_0-\frac{1}{2}\omega^2 d^2\gamma_S/dz^2}\right]^{-1}$$

$$\simeq\left[\gamma_S+\Gamma_0+\omega^2\left|\frac{(1+d\gamma_S/dz)^2}{\gamma_S+\Gamma_0}-\frac{1}{2}\frac{d^2\gamma_S}{dz^2}\right|\right]^{-1}$$

$$\simeq\frac{1}{\gamma_S+\Gamma_0}\left\{1-\frac{\omega^2}{(\gamma_S+\Gamma_0)^2}\left[\left(1+\frac{d\gamma_S}{dz}\right)^2-\tfrac{1}{2}(\gamma_S+\Gamma_0)\frac{d^2\gamma_S}{dz^2}\right]\right\}\ . \tag{B3}$$

The coefficient of the ω^2 term gives the curvature index C_2 as

$$C_2=\frac{1}{(\gamma_S+\Gamma_0)^2}\left[\left(1+\frac{d\gamma_S}{dz}\right)^2-\tfrac{1}{2}(\gamma_S+\Gamma_0)\frac{d^2\gamma_S}{dz^2}\right]\ . \tag{B4}$$

Turning now to the double Lorentzian, we have from Eq. (4.10),

$$\mathrm{Re}g_2(\omega+i\Gamma_0)=\tfrac{1}{2}(\Gamma_2+\Gamma_0)\left[\frac{1}{(\omega-\omega_2)^2+(\Gamma+\Gamma_0)^2}+\frac{1}{(\omega+\omega_2)^2+(\Gamma_2+\Gamma_0)^2}\right]$$

$$\simeq\frac{\Gamma_2+\Gamma_0}{(\Gamma_2+\Gamma_0)^2+\omega_2^2}\left[1-\frac{\omega^2}{(\Gamma_2+\Gamma_0)^2+\omega_2^2}\left[1-\frac{4\omega_2^2}{\omega_2^2+(\Gamma_2+\Gamma_0)^2}\right]\right]\ . \tag{B5}$$

The curvature coefficient C_2 is

$$C_2=\frac{1}{(\Gamma_2+\Gamma_0)^2+\omega_2^2}\left[1-\frac{4\omega_2^2}{\omega_2^2+(\Gamma_2+\Gamma_0)^2}\right]\ . \tag{B6}$$

Equating (B4) and (B6) gives, with the help of Eq. (4.12)

$$\left[1+\frac{d\gamma_S}{dz}\right]^2-\tfrac{1}{2}(\gamma_S+\Gamma_0)\frac{d^2\gamma_S}{dz^2}=\frac{(\Gamma_2+\Gamma_0)^2-3\omega_2^2}{(\Gamma_2+\Gamma_0)^2}$$
$$=1-3\frac{\gamma_S-\Gamma_2}{\Gamma_2+\Gamma_0}\ . \tag{B7}$$

A small amount of algebra puts the above equation in the form

$$\frac{1}{\Gamma_2+\Gamma_0}=\frac{1}{\gamma_S+\Gamma_0}-\frac{1}{3}\frac{1}{\gamma_S+\Gamma_0}\left[2\frac{d\gamma_S}{dz}+\left[\frac{d\gamma_S}{dz}\right]^2\right]$$
$$+\frac{1}{6}\frac{d^2\gamma_S}{dz^2}\ , \tag{B8}$$

which is the desired expression for the parameter Γ_2.

[1]R. A. Ferrell, N. Menyhárd, H. Schmidt, F. Schwabl, and P. Szépfalusy, Phys. Rev. Lett. 18, 891 (1967); Ann. Phys. (N.Y.) 47, 565 (1968).

[2]B. I. Halperin and P. C. Hohenberg, Phys. Rev. 177, 952 (1969).

[3]G. Ahlers, Phys. Rev. Lett. 21, 1159 (1968).

[4]J. A. Tyson, Phys. Rev. Lett. 21, 1235 (1968).

[5]G. Ahlers, in *The Physics of Liquid and Solid Helium,* edited by K. H. Benneman and J. B. Ketterson (Wiley, New York, 1976), Vol. I, Chap. II.

[6]J. A. Tarvin, F. Vidal, and T. J. Greytak, Phys.Rev. B 15, 4193 (1977).

[7]W. F. Vinen, C. J. Palin, J. M. Lumley, D. L. Hurd, and J. M. Vaughn, in *Low Temperature Physics, LT-14,* edited by M. Krusius and M. Vuorio (North-Holland, Amsterdam, 1975), Vol. I, p. 191.

[8]C. De Dominicis and L. Peliti, Phys. Rev. Lett. 38, 505 (1977).

[9]L. Sasvàri, F. Schwabl, and P. Szépfalusy, Physica (Utrecht) A 81, 108 (1975); and also L. Sasvàri and P. Szépfalusy, Physica (Utrecht) A 87, 1 (1977).

[10]C. De Dominicis and L. Peliti, Phys. Rev. B 18, 353 (1978).

[11]V. Dohm and R. A. Ferrell, Phys. Lett. A 67, 387 (1978).

[12]R. A. Ferrell and J. K. Bhattacharjee, J. Low Temp. Phys. 36, 1/2 (1979).

[13]V. Dohm, Z. Phys. B 33, 79 (1979).

[14]R. A. Ferrell and J. K. Bhattacharjee, Univ. of Md. Tech. Report No. 79-075 (unpublished); and Phys. Rev. Lett. 42, 1638 (1979).

[15]F. Reif, *Fundamentals of Statistical and Thermal Physics* (McGraw-Hill, New York, 1965), p. 515.

[16]A kinetic-theory treatment of the counterflow, including the noncritical background contribution as well as the velocity persistence enhancement of the thermal conductivity will appear elsewhere (unpublished).

[17]S. Chapman and T. G. Cowling, *The Mathematical Theory of Non-Uniform Gases* (Cambridge University, Cambridge, England, 1953).

[18]R. A. Ferrell, V. Dohm, and J. K. Bhattacharjee, Phys. Rev. Lett. 41, 1818 (1978).

[19]Although the combined frequency-temperature scaling property of λ has been demonstrated here only for the case where the transients are absent, we have found that it is also valid in the range where the transients are contributing to λ.

[20]R. A. Ferrell, J. Phys. (Paris) 32, 85 (1971).

[21]R. A. Ferrell and J. K. Bhattacharjee, Univ. of Md. Dept. of Phys. and Astron. Tech. Report No. 79-129, (1979) (unpublished); and *Proceedings of the Second US-USSR Symposium on the Scattering of Light by Condensed Matter,* edited by H. Cummins (Plenum, New York, 1979). See also R. A. Ferrell and J. K. Bhattacharjee, Phys. Rev. Lett. 42, 1505 (1979), for references to earlier work.

[22]P. C. Hohenberg, E. Siggia, and B. I. Halperin, Phys. Rev. B 14, 2865 (1976).